

This is the accepted manuscript made available via CHORUS. The article has been published as:

Resonant state due to Bi in the dilute bismide alloy  
 $\text{GaAs}_{1-x}\text{Bi}_x$

R. S. Joshya, A. J. Ptak, R. France, A. Mascarenhas, and R. N. Kini

Phys. Rev. B **90**, 165203 — Published 16 October 2014

DOI: [10.1103/PhysRevB.90.165203](https://doi.org/10.1103/PhysRevB.90.165203)

# Resonant state due to Bi in the dilute bismide alloy, $\text{GaAs}_{1-x}\text{Bi}_x$

R. S. Joshya,<sup>1</sup> A. J. Ptak,<sup>2</sup> R. France,<sup>2</sup> A. Mascarenhas,<sup>2</sup> and R. N. Kini<sup>1,\*</sup>

<sup>1</sup>Indian Institute of Science Education and Research Thiruvananthapuram (IISER-TVM),

CET Campus, Thiruvananthapuram, Kerala, 695016, India

<sup>2</sup>National Renewable Energy Laboratory (NREL), 1617 Cole Blvd., Golden, CO 80401, USA

## Abstract

It has been theoretically predicted that isolated Bi forms a resonant state in the valence band of the dilute bismide alloy,  $\text{GaAs}_{1-x}\text{Bi}_x$ . We present ultrafast pump-probe reflectivity measurements of this interesting alloy system which provide experimental evidence for the resonant state. The reflectivity transients for pump/probe wavelengths  $\lambda \sim 860 - 900$  nm has negative amplitude which we attribute to the absorption of the probe pulse by the pump induced carriers that are localized at the Bi resonant state. Our measurements show that the lifetime of carriers localized at the resonant state is  $\sim 200$  ps at 10K.

---

\* [rajeevkini@iisertvm.ac.in](mailto:rajeevkini@iisertvm.ac.in)

## I. INTRODUCTION

Bismuth containing III-V semiconductor alloys like  $\text{GaAs}_{1-x}\text{Bi}_x$ ,  $\text{In}_p\text{Ga}_{1-p}\text{As}_{1-q}\text{Bi}_q$ ,  $\text{GaSb}_{1-y}\text{Bi}_y$ , and  $\text{GaN}_{1-z}\text{Bi}_z$  have attracted a lot of interest in recent years due to their potential technological applications.<sup>1, 2, 3, 4, 5</sup> Of these alloys,  $\text{GaAs}_{1-x}\text{Bi}_x$  has been studied extensively and can be used in high-efficiency solar cells,<sup>6</sup> heterojunction bipolar transistors (HBTs),<sup>7</sup> spintronics<sup>8</sup> and near-infrared devices.<sup>9</sup> Bismuth containing semiconductors like  $\text{Bi}_2\text{Te}_3$  are widely used for commercial thermoelectric applications and it is known that resonant impurities increase the thermoelectric figure of merit in compound semiconductors.<sup>10</sup> In the case of  $\text{GaAs}_{1-x}\text{Bi}_x$ , it has been theoretically predicted that Bi forms a resonant state below the valence band maximum (VBM), though the exact position ( $\sim 80 - 180$  meV) of the resonant state is still under debate.<sup>11,12</sup> The presence of a resonant level might open up new avenues for applications of this interesting alloy system. However there is no experimental evidence for the resonant state due to Bi in  $\text{GaAs}_{1-x}\text{Bi}_x$ . N also introduces resonant levels in  $\text{GaAs}_{1-x}\text{N}_x$ , but in the conduction band and by applying hydrostatic pressure it was possible to push the resonant level into the gap for further study.<sup>13</sup> However, calculations have shown that the pressure co-efficient of the Bi induced resonant level in  $\text{GaAs}_{1-x}\text{Bi}_x$  is larger than that of the band gap.<sup>11</sup> Hence hydrostatic pressure studies may not yield much information about the resonant Bi level in  $\text{GaAs}_{1-x}\text{Bi}_x$ . It may be possible to study the isolated Bi level by the resonant tunnelling method<sup>14</sup> and such methods have been applied previously to study N induced resonant levels in  $\text{GaAs}_{1-x}\text{N}_x$ .<sup>15</sup> However, for resonant tunnelling studies,  $\text{GaAs}_{1-x}\text{Bi}_x$  quantum wells with very low Bi concentrations ( $x \lesssim 0.01\%$ ) are required. Controllable growth of such layers poses some practical difficulties. Ultrafast pump-probe measurements have been used to study different materials including metals, semiconductors,<sup>16</sup> magnetic materials like superconductors,<sup>17</sup> and multiferroics,<sup>18</sup> providing information about carrier, spin and phonon dynamics. It has been reported that ultrafast measurements provide

interesting information regarding the properties of materials, which cannot be obtained from continuous wave (CW) laser spectroscopy.<sup>19</sup> Even though the Bi-resonant state in  $\text{GaAs}_{1-x}\text{Bi}_x$  has been theoretically proposed several years ago, CW spectroscopy measurements have not been able to provide any experimental evidence for the same.<sup>11</sup> Here, we present results of Femtosecond pump-probe studies done on  $\text{GaAs}_{1-x}\text{Bi}_x$  epilayer and heterostructure samples which provide strong experimental evidence for the Bi-induced resonant state in the dilute bismide alloy,  $\text{GaAs}_{1-x}\text{Bi}_x$ .

## II. EXPERIMENTAL DETAILS

$\text{GaAs}_{1-x}\text{Bi}_x$  epilayers of thickness 250-300 nm were grown on semi-insulating, undoped GaAs substrates using molecular-beam epitaxy (MBE). A 250-nm thick GaAs buffer layer was grown on the substrates before growing the  $\text{GaAs}_{1-x}\text{Bi}_x$  epilayers. More details about the growth can be found in Ref [20]. We have also studied a heterostructure sample, in which a 100 nm AlAs layer was grown between the GaAs buffer layer and the 300 nm  $\text{GaAs}_{1-x}\text{Bi}_x$  epilayer. Upon excitation with NIR laser pulses, carriers are generated in both the epilayer and the buffer layer. The AlAs layer essentially blocks the carriers generated in the buffer layer from falling into the  $\text{GaAs}_{1-x}\text{Bi}_x$  well. The concentration of Bi was estimated using high-resolution x-ray diffraction (XRD) measurements and the extrapolated GaBi lattice constant of  $6.33\text{\AA}$ .<sup>21</sup> The transient reflectivity measurements ( $\Delta R/R$ ) were performed in a degenerate pump-probe arrangement using  $\sim 100$ -fs long laser pulses from a tunable Ti:Sapphire laser ( $\lambda = 740 - 950$  nm, repetition rate = 80 MHz). The pump-pulse energy is in the range 1- 9 nJ and the probe-pulse energy is about 10% of the pump energy. The pump beam was focussed on the sample to a spot of diameter  $\sim 100$   $\mu\text{m}$ . In our experiments, the changes in the reflectivity ( $\Delta R$ ) were monitored using a probe pulse which was delayed in time ( $\Delta t$ ) with respect to the pump pulse. The pump beam was mechanically chopped at  $\sim 1$

KHz and the changes in the reflectivity ( $\Delta R$ ) were recorded using a fast Si-photodiode and a lock-in amplifier.

### III. RESULTS AND DISCUSSION

Figure 1 (a) and (b) shows the transient reflectivity at different wavelengths for  $\text{GaAs}_{1-x}\text{Bi}_x$  epilayer samples with  $x = 0$  (LT-GaAs) and 3.1% respectively. As shown in Fig 1(a), at room temperature ( $\sim 300\text{K}$ ) in the LT-GaAs sample, a bi-exponential decay is observed for excitation with energy greater than the band gap ( $\lambda \lesssim 860\text{ nm}$ ). For excitation energies less than the band gap ( $\lambda > 880\text{ nm}$ ) there is a sharp negative reflectivity change, which quickly recovers and is due to intra-band transitions.<sup>22,23</sup> The transient reflectivity in  $\text{GaAs}_{1-x}\text{Bi}_x$  epilayer with  $x = 3.1\%$  shown in figure 1(b) is quite different from that observed in the LT-GaAs sample. In general, for all wavelengths there is an increase in the time required for the transient reflectivity signals to recover back to the value at  $\Delta t < 0$ . Secondly, the sign of the transient reflectivity signal is different at different wavelengths; for excitation wavelengths,  $\lambda < 840\text{ nm}$  the transient reflectivity signal is positive; for excitation wavelengths  $800\text{ nm} \lesssim \lambda < 840\text{ nm}$  there is a fast, pulse-width limited increase in reflectivity which is followed by complicated reflectivity dynamics (as shown in the inset of Fig 1(b) for  $\lambda = 800\text{nm}$ ) – an initial fast exponential decay ( $\sim 100 - 300\text{ fs}$ ), then a recovery of the transient reflectivity followed by a slow exponential decay (several tens of picoseconds). For  $840\text{ nm} \lesssim \lambda \lesssim 900\text{ nm}$  the transient reflectivity shows an initial positive amplitude but changes sign at longer delay time. For pump/probe wavelengths  $\lambda \gtrsim 920\text{ nm}$  the transient reflectivity is positive, has a slow rise time and an exponential decay.

#### *A. The three processes:*

The complicated reflectivity dynamics observed at different wavelengths can be modelled using three independent exponential relaxation processes, each with a characteristic decay

time ( $\tau_1$ ,  $\tau_2$  and  $\tau_3$ ): two of these processes have positive amplitude ( $A_1$ ,  $A_3$ ), while one of these has a negative amplitude ( $A_2$ ). To show the effectiveness of this approach in fitting the data, the different processes and the best fit to the data are shown in Fig. 2 for  $\lambda = 870$  and 900 nm.

The initial fast exponential decay ( $\tau_1 \sim 100 - 300$  fs), is caused by the thermalization of the carriers due to electron-phonon interactions and the time scale observed here is typical for III-V semiconductors<sup>24,25,26</sup>. This part of the signal may also have some significant contribution from the GaAs buffer layer and the substrate for  $\lambda \lesssim 870$  nm. This is because the thickness of these  $\text{GaAs}_{1-x}\text{Bi}_x$  films (250-300 nm) is close to the absorption length of light at these wavelengths and some amount of pump pulse is absorbed in the buffer and substrate underneath. The carriers created in the buffer and the substrate may fall into the  $\text{GaAs}_{1-x}\text{Bi}_x$  layer which has a smaller band gap compared to GaAs and contribute to the reflectivity change. At excitation energies below the band gap of GaAs ( $\lambda > 870$  nm) there is no absorption from the buffer layer and the substrate; hence the signal is predominantly from the  $\text{GaAs}_{1-x}\text{Bi}_x$  layer. The picoseconds long exponential decay ( $\tau_3 \sim 10 - 150$  ps) is due to the recombination of the photoexcited carriers via defects. In general, III-V semiconductors doped with isoelectronic dopants like N and Bi show very long recombination time.<sup>27, 28</sup> Photoluminescence (PL) experiments have shown that in GaAsBi the radiative recombination occurs on a nanosecond time scale ( $\sim 50 - 80$  ns).<sup>29,30</sup> Since the laser pulse repeats every 12 ns, the radiative recombination process is not probed in our measurements and the observed lifetime  $\tau_3$  corresponds to the faster recombination via defects. The intermediate decay process ( $A_2$ ,  $\tau_2$ ) has a negative amplitude and we will discuss the origin of this process in the rest of this paper. Taking into account these three processes we were able to fit our observed data for different wavelengths quite well. The wavelength region where the negative transient reflectivity is observed can be more clearly seen in the contour plot shown in Fig. 3 (a). The

picosecond-long negative transients were observed only in GaAs<sub>1-x</sub>Bi<sub>x</sub> epilayers with  $x=1.4\%$  (not shown) and 3.1% and heterostructure sample (discussed later). In order to understand the origin of the negative transient reflectivity, we analysed our data based on Kramers-Kronig relations. We will discuss this in the next section.

### *B. Kramers-Kronig analysis*

The photoexcitation of a semiconductor with an ultrashort laser pulse results in the creation of electron-hole pairs. The photoexcited carriers cause changes in the complex refractive index  $\Delta\tilde{n} = \Delta n + i\Delta k$  and consequently changes in the reflectivity ( $\Delta R$ ).  $\Delta R/R$  is directly proportional to  $\Delta n$ :<sup>31</sup>

$$\frac{\Delta R}{R} \approx 4 \frac{\Delta n}{n^2 - 1}$$

where  $n$  and  $R$  is the background refractive index and reflectivity respectively. The time evolution of  $\Delta n$  and hence  $\Delta R$  essentially follow the decay of the photoexcited carriers. The real and imaginary parts of the refractive index are related by Kramers-Kronig integrals, according to which the change in refractive index due to photoexcited carriers,  $\Delta n(\Delta t)$  at a particular energy,  $E$  can be written as,<sup>32</sup>

$$\Delta n(E, \Delta N, \Delta t) = \frac{c\hbar}{\pi} P \int_0^\infty \frac{\Delta\alpha(E', \Delta N)}{E'^2 - E^2} dE'$$

where  $P$  denotes the principal value of the integral,  $\Delta\alpha(E, \Delta N) = \alpha(E, \Delta N) - \alpha(E, 0)$  is the change in absorption coefficient,  $\alpha = \frac{2kE}{\hbar c}$  at a particular photon energy,  $E$ ,  $c$  is the speed of light and  $\hbar$  is the reduced Planck's constant. This equation shows that for a positive peak in  $\Delta\alpha(E)$ ,  $\Delta n$  is negative for energies above the peak and  $\Delta n$  is positive for energies below the

peak. Using this equation we have calculated  $\Delta n$  for different wavelengths, assuming an absorption peak at  $\lambda = 885$  nm as shown in the inset of Fig. 3(b). We have taken into account the bandwidth of the laser pulse ( $\sim 33$  meV) and assumed that the absorption peak appears only when the photon energy is greater than the energy of the peak in  $\Delta\alpha$ . The  $\Delta n$ -vs- $\lambda$  curve shown in Fig. 3(b) qualitatively agrees with the amplitude of negative process,  $A_2$  -vs-  $\lambda$  curve. This suggests that the negative amplitude process is due to an absorption peak.

It is known that Bi in GaAs creates a resonant state and bound states for holes due to isolated Bi impurities and Bi-Bi pairs/clusters respectively. The pump generated carriers become localized at these states as shown schematically in Fig. 4 and these carriers can induce absorption. Negative transient reflectivity due to induced absorption caused by trapped carriers has been observed before in strongly correlated electron systems<sup>17</sup> and low-temperature grown III-V semiconductors.<sup>33</sup> This simple model which gives good agreement with the data suggests that the negative transient region is due to induced absorption.

The negative transient region shown in Fig 3(a) is very close to the band gap of GaAs. As mentioned earlier, upon photo-excitation carriers are created in the GaAs buffer and substrate also. The band gap of the  $\text{GaAs}_{1-x}\text{Bi}_x$  epilayer is lower than the GaAs buffer layer/substrate. Hence the epilayer essentially forms a potential well for the carriers generated by the NIR pulses in the buffer and substrate layer. These carriers fall into  $\text{GaAs}_{1-x}\text{Bi}_x$  well and also contribute to the reflectivity dynamics. This raises the question whether the induced absorption is due to the carrier generated in the GaAs buffer layer/substrate. In order to separate the effect of the carriers generated in the buffer layer/substrate from those generated in the  $\text{GaAs}_{1-x}\text{Bi}_x$  layer, we studied the hetero-structure sample. The hetero-structure sample had an AlAs layer between the  $\text{GaAs}_{1-x}\text{Bi}_x$  epilayer and the GaAs buffer layer. The AlAs layer blocked the carriers generated in the buffer layer from falling into the  $\text{GaAs}_{1-x}\text{Bi}_x$  well.



The hetero-structure sample had a Bismuth concentration of  $x = 2.7\%$ , very close to the concentration in the epilayer sample discussed above. The small difference in Bismuth concentration between the epilayer and heterostructure sample will cause a blue-shift of the band gap of the heterostructure sample by about 35 meV compared to the epilayer sample discussed earlier. Since the pump photon energies are well above the band gap energy, we do not expect this small change in band gap to affect our measurements. Contour plot of  $\Delta R/R$  for  $\lambda - \Delta t$  grid for the  $\text{GaAs}_{1-x}\text{Bi}_x$  hetero-structure sample is shown in Fig. 5(a) and (b) for measurements done at 300 K and 10 K respectively. At 300 K, the wavelength region where the negative reflectivity transients are observed is similar to that observed in the epilayer sample and very close to the band gap of GaAs at 300 K. At low temperatures ( $\sim 10 - 20$  K) the relaxation time of the negative amplitude process increases as evident from Fig. 5(b). However, the negative amplitude region does not shift significantly in energy ( $\sim 16$  meV), whereas the GaAs band gap shifts up by about 95 meV. This, along with the fact that the negative amplitude process is not observed in GaAs allows us to discount the possibility that the negative transient is due to the GaAs buffer layer or substrate. The calculated  $\Delta n$ -vs- $\lambda$  curves qualitatively agree with the measured  $A_2$ -vs- $\lambda$  curves as shown in Fig. 5 (c) and (d). The  $\Delta n$ -vs- $\lambda$  curves were calculated assuming an absorption peak at  $\lambda = 900$  nm and 885 nm for 300 K and 10 K respectively. The good agreement between the calculated and experimental curves confirms that the negative transient region is due to induced absorption caused by carriers trapped at Bi-related states in  $\text{GaAs}_{1-x}\text{Bi}_x$ . We have used the Kramers-Kronig relation to simulate the dynamics of the carriers, as shown for the heterostructure sample in Fig 6 (a) & (b) for 300K and 10K respectively. For 300K, we have used  $\tau_2 = 50$  ps and for 10K we have used  $\tau_2 = 200$  ps and for simplicity we have used the same  $\tau_2$  across different wavelengths. The simulated contour plot of  $\Delta n$  for  $\lambda - \Delta t$  grid qualitatively matches

well with the data in Fig 5 (a) & (b) and shows that the carriers are trapped at the Bi related state for hundreds of picoseconds at low temperatures.

### *C. Temperature and power dependence.*

To further confirm that the negative amplitude region is due to Bi related state, we performed temperature and power dependant measurements on the heterostructure sample. Figure 7 (a) shows the negative transient region in the heterostructure sample at different temperatures and Fig. 7 (b) shows the corresponding simulated data. From the experimental data it can be seen that the negative transient region shifts to lower energies as the temperature is increased. From the simulated data we have obtained the energy of the peak in  $\Delta\alpha$  as a function of temperature and is plotted in Fig. 7 (c). In the high temperature range the peak energy shifts at the rate of  $-0.17$  meV/K, which is close to the value of the band gap reduction with increasing temperature in  $\text{GaAs}_{1-x}\text{Bi}_x$  at these Bi compositions.<sup>34</sup> In contrast the bandgap of GaAs decreases with increase in temperature at the rate of  $\sim 0.42$  meV/K. This further confirms that the negative amplitude region is due to the Bi related state and the reduction in the temperature sensitivity of the bandgap of the dilute Bismide alloy  $\text{GaAs}_{1-x}\text{Bi}_x$  is due to the presence of this state. As the temperature is decreased the thermal emission of trapped carriers is reduced<sup>35</sup> and hence we observe an increase in the lifetime,  $\tau_2$  at lower temperatures as shown in Fig. 7 (b).

Figure 7 (d) shows the amplitude of the negative process at 12 K (300K) for different excitation pump power at a pump/probe wavelength of  $\sim 865$  nm (880 nm). We see an almost linear increase in the amplitude of the negative process with increase in pump pulse energy. Even at the highest pump pulse energy, where we expect a photo-generated carrier density of  $\sim 2 \times 10^{18} \text{ cm}^{-3}$ , we do not see any saturation of the negative process which implies that the density of the trap states responsible for this is much greater than  $10^{18} \text{ cm}^{-3}$ . The

concentration of unintentional impurities and defects will be less than  $10^{18} \text{ cm}^{-3}$ , whereas the trap states due to isolated Bi and Bi-Bi pairs will be  $\sim 10^{19} - 10^{20} \text{ cm}^{-3}$ . Hence the power dependant data also confirms our earlier conclusion that negative amplitude process is due to the Bi related state.

From previous measurements we can estimate the band gap of  $\text{GaAs}_{1-x}\text{Bi}_x$  with  $x = 2.7\%$  to be  $\sim 1.195 \text{ eV}$  at 300 K and  $1.24 \text{ eV}$  at 10 K.<sup>36</sup> Hence the trap state responsible for the induced absorption peak at  $\lambda \sim 900 \text{ nm}$  ( $E \sim 1.378 \text{ eV}$ ) at room temperature and  $\lambda \sim 885 \text{ nm}$  ( $E \sim 1.4 \text{ eV}$ ) at 10 K will be resonant, most likely in the valence band as shown schematically in Fig. 4. Bi incorporation in GaAs mainly perturbs the valence band (VB), with little or no effect on the conduction band (CB) and creates a resonant state in the VB due to isolated Bi and bound states due to Bi-Bi pairs/clusters. Considering this, it is unlikely that the resonant state responsible for the induced absorption is in the CB. Hence we attribute the negative transient reflectivity to induced absorption by pump generated carriers trapped at the resonant state in the VB due to isolated Bi impurities.

#### IV. CONCLUSIONS

In summary, we have performed time-resolved reflectivity measurements on epilayers and heterostructures of the dilute bismide alloy,  $\text{GaAs}_{1-x}\text{Bi}_x$ . Our measurements provide experimental evidence for a resonant state due to Bi in  $\text{GaAs}_{1-x}\text{Bi}_x$ . The transient reflectivity signal has negative amplitude in the pump/probe wavelength region near  $\lambda \sim 860 - 900 \text{ nm}$ . We attribute this to the absorption of the probe pulse by the pump induced carriers that are trapped at the Bi resonant level. The carriers are trapped at the Bi resonant state for hundreds of picoseconds at low temperatures.

*Acknowledgments:*

The authors thank Brian Fluegel and Yong Zhang for useful discussions and critical reading of the manuscript. Research at IISER-TVM was supported by Science and Engineering Research Board, Department of Science and Technology, India through the Fast Track Scheme for Young Scientists and the sample growth at NREL was supported by U.S. Department of Energy, Basic Energy Sciences, Materials Sciences and Engineering Division under contract no. DE-AC36-08GO28308.

## Figure Captions

Figure 1. The transient reflectivity at 300K for different pump/probe wavelengths for  $\text{GaAs}_{1-x}\text{Bi}_x$  epilayer samples with (a)  $x = 0$  and (b)  $x = 3.1\%$ . The traces are offset vertically for clarity. These measurements were done with pump pulses of energy  $\sim 3.8$  nJ. The inset of (b) shows the data obtained for  $\lambda = 800$  nm on a smaller time scale.

Figure 2. The different decay processes and the best fit to the data for  $\text{GaAs}_{1-x}\text{Bi}_x$  epilayer sample at 300K for pump/probe wavelength, (a)  $\lambda = 900$  nm and (b)  $\lambda = 870$  nm.

Figure 3. Contour plot of  $\Delta R/R$  for  $\lambda - \Delta t$  grid for the  $\text{GaAs}_{1-x}\text{Bi}_x$  epilayer sample with  $x = 3.1\%$  at 300 K. (b) The amplitude of the negative transient reflectivity  $A_2$  and calculated  $\Delta n$  is plotted against  $\lambda$  for the epilayer sample. The inset shows the shape of the  $\Delta\alpha$  curve used for calculating the  $\Delta n$  curve.

Figure 4. A schematic representation of the various bands - Conduction Band (CB), Light hole/Heavy hole (LH/HH) bands, Spin split-off (SO) band and the resonant state due to Bi - is shown along with the non-equilibrium carrier distribution at different time scales.

Figure 5. Contour plot of  $\Delta R/R$  for  $\lambda - \Delta t$  grid for the  $\text{GaAs}_{1-x}\text{Bi}_x$  hetero-structure sample with  $x = 2.7\%$  for (a) 300 K and (b) 10 K. (c) The amplitude of the negative transient reflectivity  $A_2$  and calculated  $\Delta n$  is plotted against  $\lambda$  for the hetero-structure sample. The inset shows the shape of the  $\Delta\alpha$  curve used for calculating the  $\Delta n$  curve. (d) Data same as (c) but for 10K. These measurements were done with pump pulses of energy  $\sim 6.3$  nJ

Figure 6. Contour plot of the calculated  $\Delta n$  for  $\lambda - \Delta t$  grid, using  $\tau_2 = 50$  ps and 200 ps for the  $\text{GaAs}_{1-x}\text{Bi}_x$  hetero-structure sample with  $x = 2.7\%$  at (a) 300 K and (b) 10 K respectively.

Figure 7. (a) Contour plot of  $\Delta R/R$  for  $\lambda - \Delta t$  grid for the  $\text{GaAs}_{1-x}\text{Bi}_x$  hetero-structure sample with  $x = 2.7\%$  for different temperatures. These measurements were done with pump pulses

of energy  $\sim 6.3$  nJ (b) The corresponding contour plots of the calculated  $\Delta n$  for  $\lambda - \Delta t$  grid. (c) Position of the peak in  $\Delta\alpha$  used for calculating  $\Delta n$  at different temperatures. The straight line is a linear fit to the high temperature region (150-300K) of the data (d) Amplitude of the negative transients for  $\lambda = 865$  nm (880 nm) for 10 K (300K) for different pump pulse energies.

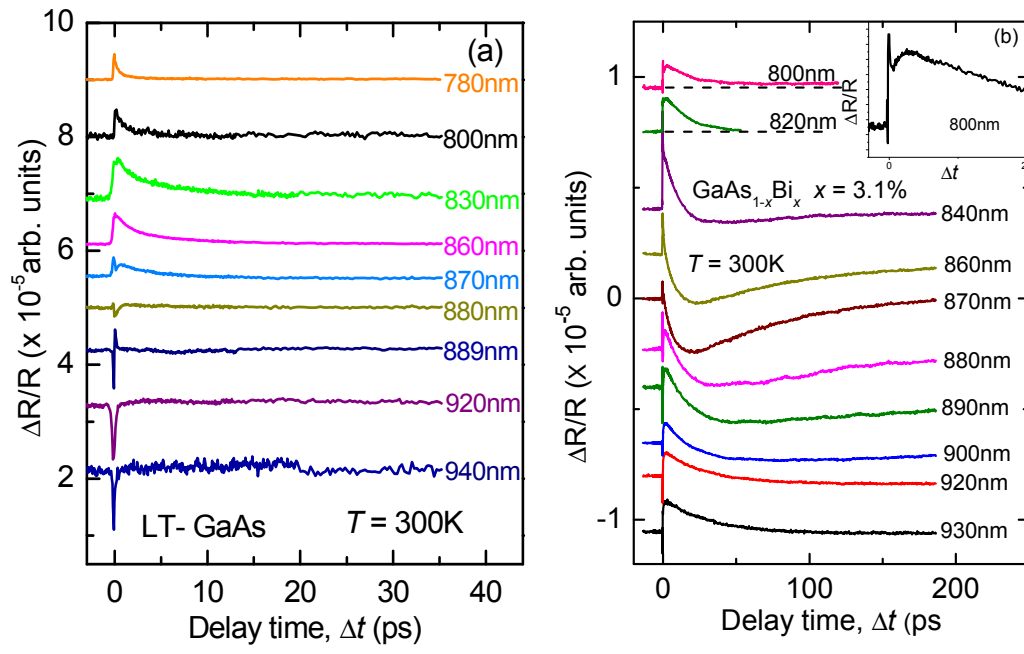


Figure 1

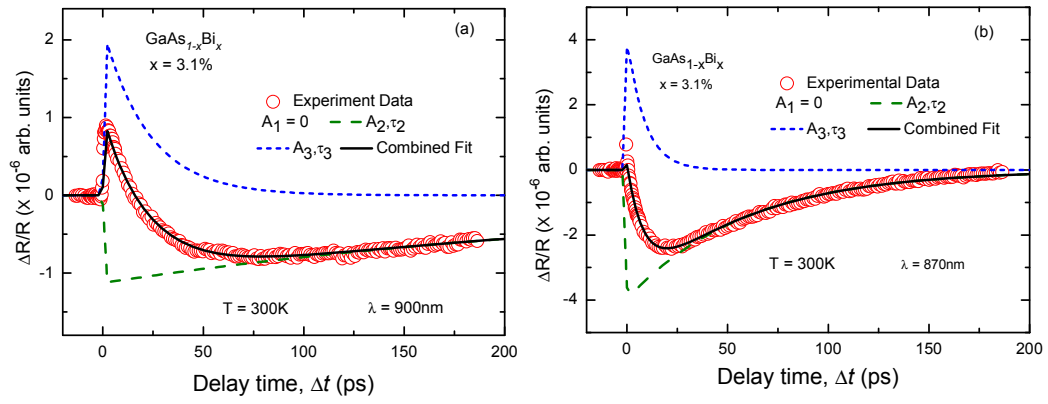


Figure 2



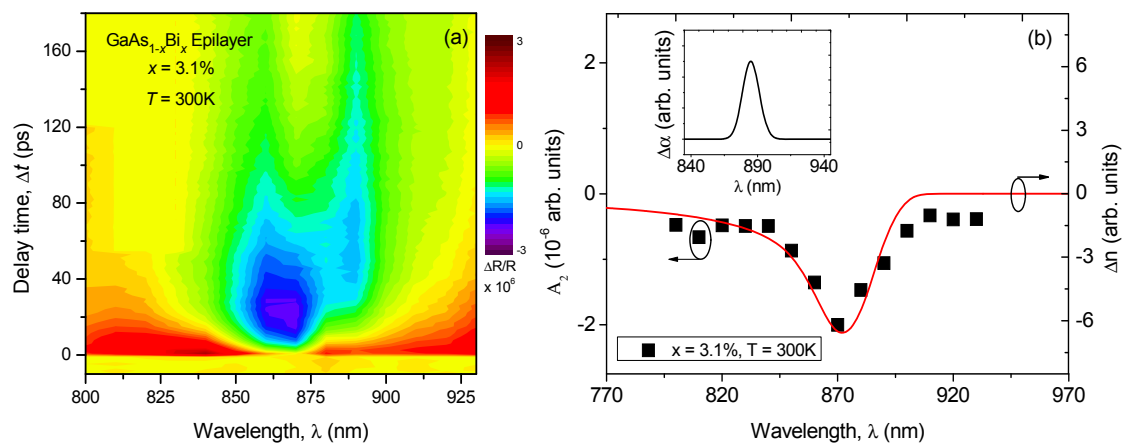


Figure 3

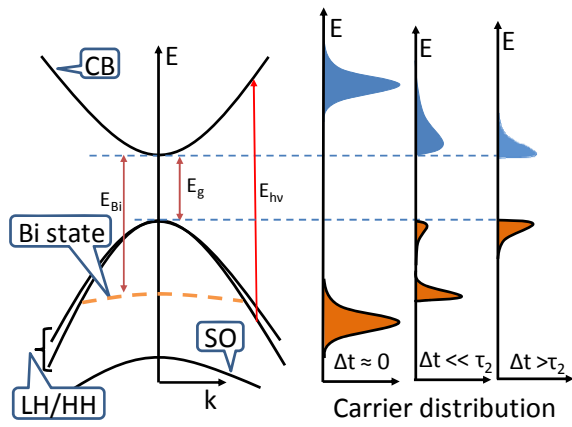


Figure 4

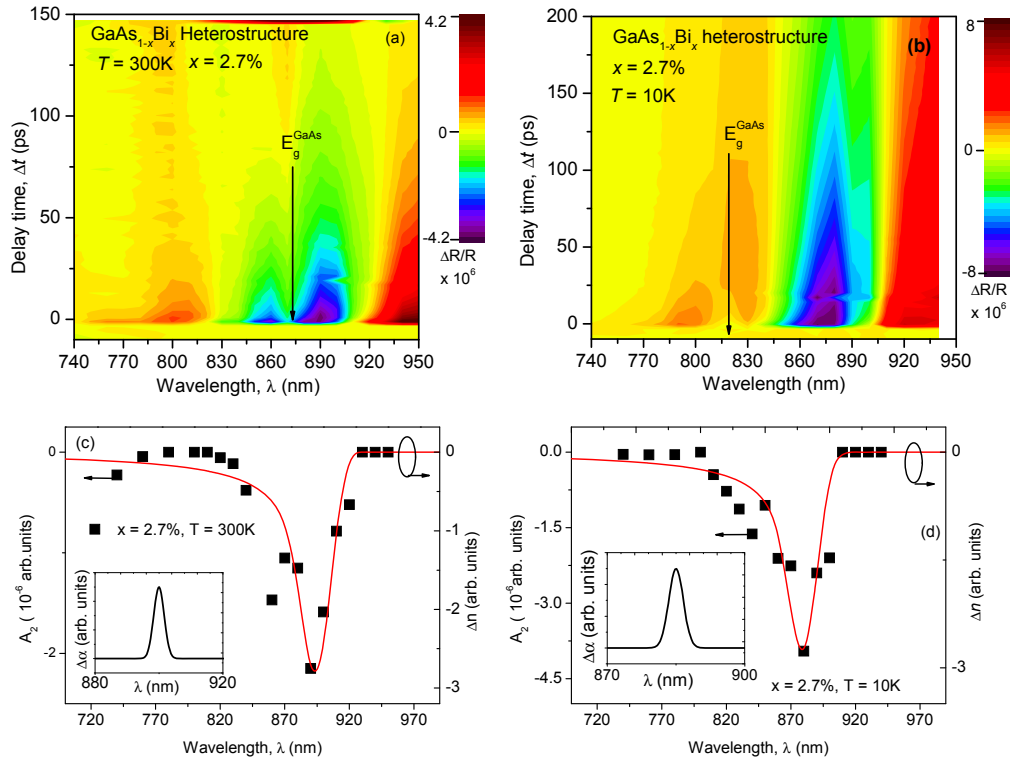


Figure 5

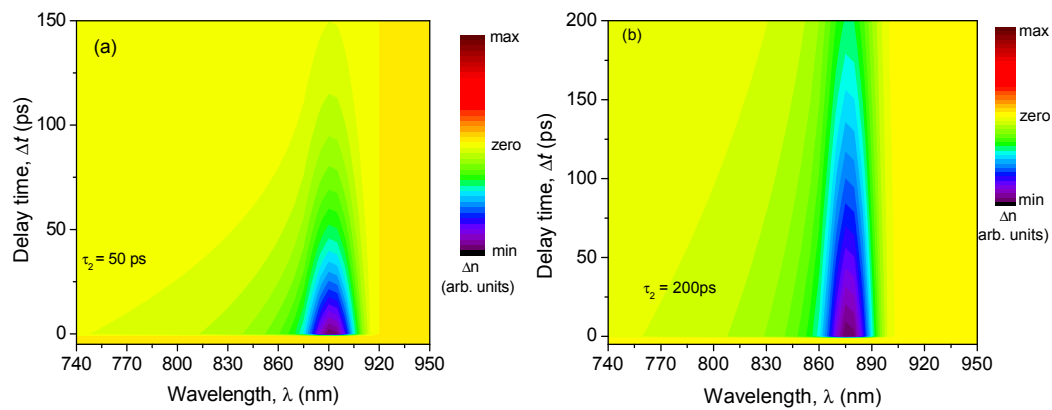
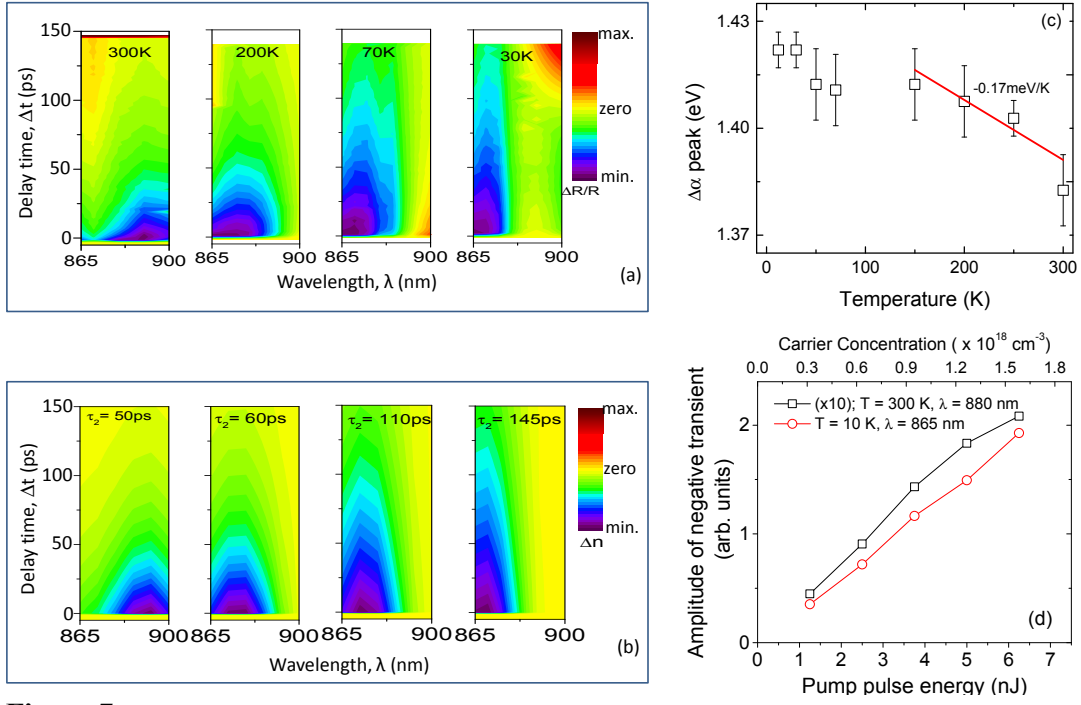


Figure 6



**Figure 7**

## References:

- 
- <sup>1</sup> S. Francoeur, M.-J. Seong, A. Mascarenhas, S. Tixier, M. Adamczyk, and T. Tiedje, Appl. Phys. Lett. 82, 3874 (2003)
- <sup>2</sup> B. Fluegel, S. Francoeur, A. Mascarenhas, S. Tixier, E. C. Young, and T. Tiedje, Phys. Rev. Lett. 97, 067205 (2006)
- <sup>3</sup> A. X. Levander, K. M. Yu, S. V. Novikov, A. Tseng, C. T. Foxon, O. D. Dubon, J. Wu, and W. Walukiewicz, Appl. Phys. Lett. 97, 141919 (2010)
- <sup>4</sup> J. P. Petropoulos, Y. Zhong, and J. M. O. Zide, Appl. Phys. Lett. 99, 031110 (2011)
- <sup>5</sup> S.K. Das, T.D. Das, S. Dhar, M. de la Mare, A. Krier, Infrared Physics & Technology 55, 156 (2012)
- <sup>6</sup> F. Dimroth, Phys. Stat. Sol. (c) 3, 373 (2006)
- <sup>7</sup> P M Asbeck, R J Welty, C W Tu, H P Xin and R E Welser, Semicond. Sci. Technol, 17, 898 (2002)
- <sup>8</sup> H. Tong, X. Marie, and M. W. Wu, J. Appl. Phys. 112, 063701 (2012)
- <sup>9</sup> N. Hossain, I. P. Marko, S. R. Jin, K. Hild, S. J. Sweeney, R. B. Lewis, D. A. Beaton, and T. Tiedje, Appl. Phys. Lett. 100, 051105 (2012)
- <sup>10</sup> J. P. Heremans, B. Wiendlocha and A. M. Chamoire, Energy Environ. Sci., 5, 5510 (2012)
- <sup>11</sup> Y. Zhang, A. Mascarenhas, and L.-W. Wang, Phys. Rev. B 71, 155201 (2005)
- <sup>12</sup> M. Usman, C. A. Broderick, A. Lindsay, and E. P. O'Reilly, Phys. Rev. B 84, 245202 (2011)
- <sup>13</sup> D. J. Wolford, J. A. Bradley, K. Fry, J. Thompson, and H. E. King, in Proceedings of the 17th International Conference on the Physics of Semiconductors, edited by J. D. Chadi and W. A. Harrison (Springer, New York, 1984), p. 627.
- <sup>14</sup> R. K. Hayden, D. K. Maude, L. Eaves, E. C. Valadares, M. Henini, F. W. Sheard, O. H. Hughes, J. C. Portal, and L. Cury, Phys. Rev. Lett. 66, 1749–1752 (1991)
- <sup>15</sup> J. Endicott, A. Patané, J. Ibáñez, L. Eaves, M. Bissiri, M. Hopkinson, R. Airey, and G. Hill, Phys. Rev. Lett. 91, 126802 (2003)
- <sup>16</sup> J Wang, C Sun, Y Hashimoto, J Kono, G A Khodaparast, Ł Cywiński, L J Sham, G D Sanders, C J Stanton and H Munekata, J Phys. Condens. Matter, 18 R501 (2006)
- <sup>17</sup> J. Qi, X. Chen, W. Yu, P. Cadden-Zimansky, D. Smirnov, N. H. Tolk, I. Miotkowski, H. Cao, Y. P. Chen, Y. Wu, S. Qiao, and Z. Jiang, Appl. Phys. Lett. 97, 182102 (2010)
- <sup>18</sup> J. Lee, S. A. Trugman, C. D. Batista, C. L. Zhang, D. Talbayev, X. S. Xu, S.-W. Cheong, D. A. Yarotski, A. J. Taylor and R. P. Prasankumar, Scientific Reports 3, 2654 (2013)
- <sup>19</sup> C. Liu, N. M. Dissanayake, S. Lee, K. Lee, and Z. Zhong, ACS Nano, 6, 7172 (2012)
- <sup>20</sup> R. N. Kini, L. Bhusal, A. J. Ptak, R. France, and A. Mascarenhas, J. Appl. Phys. 106, 043705 (2009)

- 
- <sup>21</sup> S. Tixier, M. Adamczyk, T. Tiedje, S. Francoeur, A. Mascarenhas, P. Wei, and F. Schiettekatte, Appl. Phys. Lett. 82, 2245 (2003)
- <sup>22</sup> T. Gong, W. L. Nighan, and P. M. Fauchet, Appl. Phys. Lett. 57, 2713 (1990)
- <sup>23</sup> J. P. Zahn, A. Gamouras, S. March, X. Liu, J. K. Furdyna, and K. C. Hall, J. Appl. Phys. 107, 033908 (2010);
- <sup>24</sup> S. Janz, Usman G. Akano, and Ian V. Mitchell, Appl. Phys. Lett. 68, 3287 (1996)
- <sup>25</sup> T. S. Sosnowski, T. B. Norris, H. H. Wang, P. Grenier, J. F. Whitaker et al., Appl. Phys. Lett. 70, 3245 (1997)
- <sup>26</sup> Muneaki Hase, Kunie Ishioka, Masahiro Kitajima, and Kiminori Ushida, Appl. Phys. Lett. 82, 3668 (2003)
- <sup>27</sup> W. Rühle, W. Schmid, R. Meck, N. Stath, J. U. Fischbach, I. Strottner, K. W. Benz, and M. Pilkuhn, Phys. Rev. B 18, 7022 (1978)
- <sup>28</sup> J. D. Cuthbert and D. G. Thomas, Phys. Rev. 154, 763 (1967)
- <sup>29</sup> R. N. Kini, A. Mascarenhas, R. France, and A. J. Ptak, J. Appl. Phys. 104, 113534 (2008)
- <sup>30</sup> S Imhof, C Wagner, A Thränhardt, A Chernikov, M Koch, N S. Köster, S Chatterjee, S W. Koch, O Rubel, X Lu, S R. Johnson, D A. Beaton, and T Tiedje, Appl. Phys. Lett. 98, 161104 (2011)
- <sup>31</sup> A. J. Sabbah and D. M. Riffe, Phys. Rev. B 66, 165217 (2002)
- <sup>32</sup> O. Madelung, Introduction to Solid State Theory (Springer-Verlag, Berlin, 1981)
- <sup>33</sup> U. Siegner, R. Fluck, G. Zhang, and U. Keller, Appl. Phys. Lett. 69, 2566 (1996)
- <sup>34</sup> J. Yoshida, T. Kita, O Wada and K. Oe, Jpn. J. Appl. Phys. 42, 371 (2003)
- <sup>35</sup> S. Gupta, P. K. Bhattacharya, J. Pamulapati, and G. Mourou, Appl. Phys. Lett. 57, 1543 (1991)
- <sup>36</sup> R. N. Kini, A. J. Ptak, B. Fluegel, R. France, R. C. Reedy, and A. Mascarenhas, Phys. Rev. B 83, 075307 (2011)